Surface & Coatings Technology 309 (2017) 872–879

Contents lists available at ScienceDirect

Surface & Coatings Technology

journal homepage: www.elsevier.com/locate/surfcoat

Flame spray fabrication of polyethylene-Cu composite coatings with enwrapped structures: A new route for constructing antifouling layers

Zhengmei Jia [a,b], Yi Liu [b], Yingying Wang [c], Yongfeng Gong [b], Peipeng Jin [a], Xinkun Suo [b,*], Hua Li [b,*]

[a] School of Mechanical Engineering, Qinghai University, Xining 810016, China
[b] Key Laboratory of Marine Materials and Related Technologies, Zhejiang Key Laboratory of Marine Materials and Protective Technologies, Ningbo Institute of Materials Technology and Engineering, Chinese Academy of Sciences, Ningbo 315201, China
[c] College of Chemistry and Chemical Engineering, Southwest Petroleum University, Chengdu 610500, China

ARTICLE INFO

Article history:
Received 14 July 2016
Revised 24 October 2016
Accepted in revised form 25 October 2016
Available online 27 October 2016

Keywords:
HDPE-Cu composites
Antifouling
Anti-corrosion
Electroless plating
Flame spraying

ABSTRACT

Biofouling and corrosion are predominant worldwide concerns in modern marine industries. Large-scale fabrication of protective coatings against both corrosion and biofouling yet remains elusive. Here we propose a new technical route for constructing inorganic/organic composite coatings for promising anti-corrosion and long-term antifouling performances. Electroless plating was employed for making copper (Cu)-high density polyethylene (HDPE) core-shell particles for following coating deposition by flame spraying. Copper shells with a thickness of ~1 μm surrounding individual HDPE particles were obtained. Homogeneously distributed thin copper layers existing at the interfaces of HDPE splats did not deteriorate corrosion resistance of the HDPE coatings as assessed by electrochemical testing. Neutral salt spray testing for 14 days reveals almost intact state of the coatings. Electrochemical results show that the HDPE-Cu coatings have better corrosion resistance. Significantly constrained attachment of *Bacillus* sp. bacteria on the surfaces of the Cu-containing coatings was observed, suggesting their excellent antifouling performances. Continuous release in low-dose of copper ions confers long-term antifouling capability on the coatings. The strategy for fabricating the novel HDPE-Cu coatings gives bright insight into their potential antifouling applications in the marine environment.

1. Introduction

Marine biofouling is an undesirable phenomenon brought about by marine organisms occurred on a surface immersed in seawater [1]. It usually gives rise to a variety of problems, e.g. increased fuel consumption of ships, microbiologically induced corrosion, pipe blockage, signal distortion of instruments, etc. Antifouling technologies for marine structures have therefore been explored extensively in past decades [2,3]. To date, one of the most effective solutions to the fouling problem is treating the surface with an antifouling layer [4,5]. This usually involves the use of biocides as the key coating component. Antifouling techniques based on biocides are well-established for effectively preventing biofouling for marine infrastructures. Copper has become the most important alternative biocide since organotin compounds were banned. Various copper agents including copper alloys, cuprous oxide and copper compounds have been used as principal biocides for decades [6,7]. As it is challenging to apply biocides on substrate surfaces directly for long-term services, developing appropriate techniques for incorporating biocides into coatings has been one of the recent research efforts. The major concerns pertaining to the fabrication of biocides-containing coatings are controllable release of the biocides and sufficient anti-corrosion performances.

Corrosion resistance is a crucial requirement of marine protective coatings, which restricts their service time. Among the surface coating techniques for marine applications, thermal spraying has been extensively used to fabricate anti-corrosion layers. Thermal sprayed metallic coatings (e.g. aluminum, zinc and aluminum-zinc alloy coatings) have shown long-term corrosion protection for steel structures in the marine environment for more than 20 years [8–10]. Thermal sprayed polymer coatings like high density polyethylene (HDPE), low-density polyethylene (LDPE) [11], ultra-high molecular weight polyethylene (UHMWPE) [12] and high quality poly-ether-ether-ketone (PEEK) [13,14] have proven to perform well in the corrosive environment. However, it is difficult to involve the copper biocide in the metallic coatings due to galvanic corrosion between the metallic constituents. Therefore, appropriate addition of biocides into the polymer coatings might be a promising way to fabricate anti-corrosion and antifouling coatings for marine applications.

In fact, there have been attempts in recent years of using copper to construct antifouling layers by thermal spraying. Antifouling performances of cold sprayed Cu/Cu_2O inorganic coatings have been reported by Ding et al. and increased Cu_2O content brought about enhanced antifouling performances [15]. Yet, the coatings do not offer the capability

* Corresponding authors.
E-mail addresses: suoxinkun@nimte.ac.cn (X. Suo), lihua@nimte.ac.cn (H. Li).

http://dx.doi.org/10.1016/j.surfcoat.2016.10.071
0257-8972/

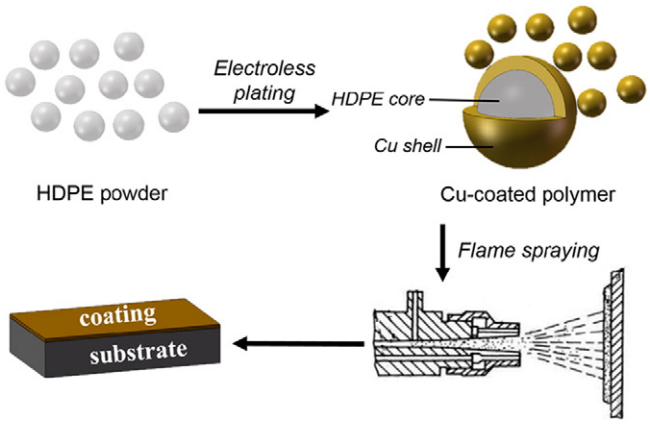

Fig. 1. Schematic depiction illustrating the fabrication route for the HDPE-Cu antifouling coatings deposited by flame spraying.

to resist corrosion. Embedding of copper particles by cold spraying into polymer [16] might avoid the deficiency in corrosion resistance, while facilitate the antifouling performances by impeding attachment of marine organisms through release of copper ions from the composite structure. Further investigations on bronze and zinc embedded structures revealed similar antifouling performances [17–19]. However, the thin layer of the composite structure achieved by embedding metal particles into the polymer matrix would influence release efficiency and potential application of the structure against biofouling. Cost-efficient fabrication of large-scale anti-corrosion/fouling polymer-based coatings is to be further explored. Taking into account the fact that use of copper is still permitted for antifouling purposes, appropriate preparation of the starting polymer-Cu composites is essential for developing consequent antifouling coatings.

Thermal sprayed coatings for marine applications have been extensively investigated, however, few of them satisfy both sufficient anticorrosion and antifouling properties. Therefore, in this study, the coatings with excellent corrosion resistance and promising antifouling property were developed. The microstructure, corrosion resistance and antifouling properties of the novel coatings were characterized and elucidated. Distribution of copper biocides in the coatings and controllable release of copper ions were also investigated.

2. Materials and methods

Commercially available HDPE powder (Korea Petrochemical Ind. Co., Ltd) was used as the starting feedstock. Size distribution of the powder

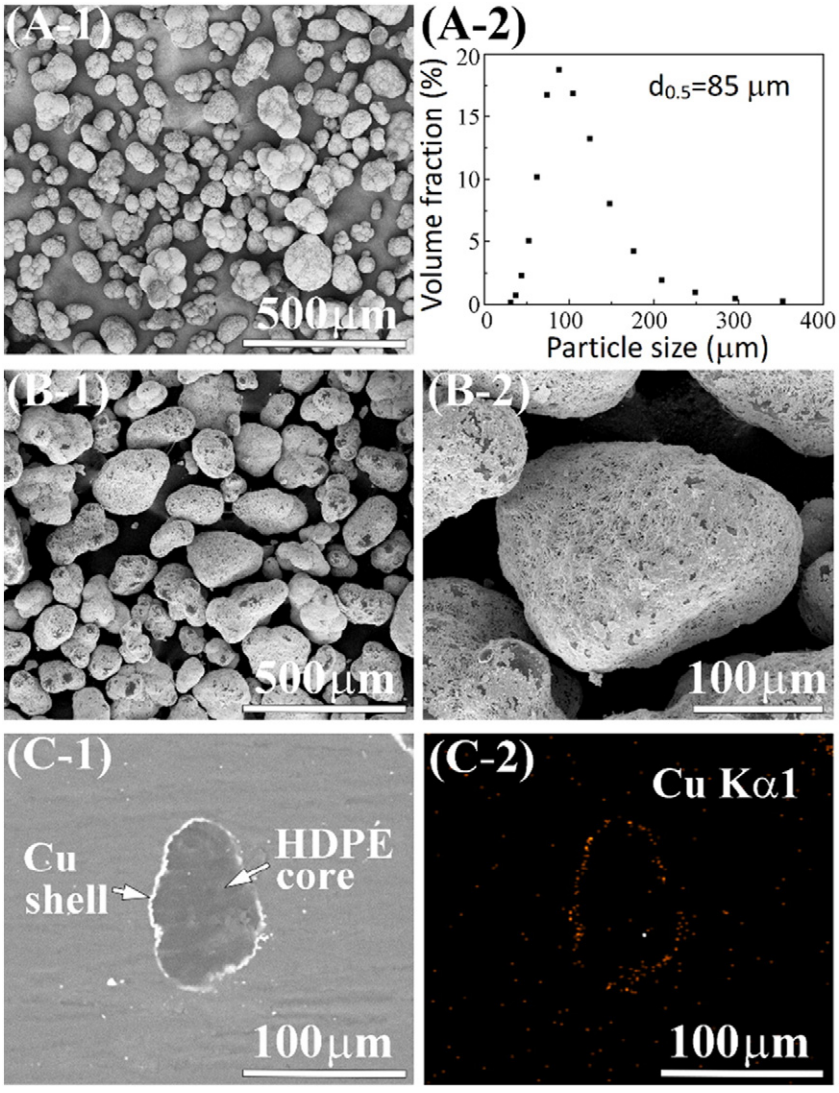

Fig. 2. Surface morphology (A-1) and particle size distribution (A-2) of the starting HDPE powder, topographical views of the electroless plated HDPE-Cu particles (B-1, B-2), and cross-sectional view of single HDPE-Cu particle and EDS mapping analysis for the Cu layer (C-1, C-2).

was measured using a commercial particle size analyzer (Microtrac, S3500-special, USA). Supersonic treatment was conducted during the measurement to break up the possibly agglomerate particles. To construct the HDPE-based coatings for anti-fouling/corrosion performances, a special processing route was designed for preparing the starting HDPE-Cu powder and their coatings. The route for making the HDPE-Cu coatings is schematically depicted in Fig. 1. To achieve a desirable coating structure, prior to the spraying, a thin Cu wrapping layer was deposited to enwrap the HDPE particle by electroless plating. Pretreatment procedures of the HDPE powder have been reported by other researchers previously [20]. A solution of $CuSO_4$ in deionized water with a concentration of 20 g/L was used as a plating bath. HDPE powder was added into the plating bath at 50 °C for 40 mins. Thickness of the copper shell surrounding HDPE particle was tunable by changing electroless plating cycles.

Copper (BGRIMM Advanced Materials Science & Technology Co., Ltd, average diameter/$d_{0.5}$ = 18.71 μm), HDPE and the Cu-coated HDPE particles were deposited respectively on mild steel plates (MS, E235B, 20 × 30 × 2 mm^3) by flame spraying (CDS 8000, Castolin, UK). Before the coating deposition, the MS substrates were cleaned in turn by acetone, hydrochloric acid and deionized water, and then mechanically coarsened by sand blasting with alumina. Oxygen and acetylene were used as the combustion-supporting gas and fuel gas with the pressure of 0.55 MPa and 0.075 MPa, respectively. Feed rate of the powder was set as 60 g/min. The standoff distance from nozzle exit to sample surface was 250 mm. Traverse speed of the gun was 200 mm/s.

The microstructures of the powder and the coatings were characterized by field emission scanning electron microscope (FESEM, Quanta FEG 250, USA). Distribution of copper in the coatings was analyzed using energy dispersive spectrometer (EDS) equipped with FESEM. The phase composition of the samples was examined by X-ray diffraction (XRD, D8 Advance, Bruker AXS, Germany) at a scanning rate of 0.1°/s using Cu Kα radiation operated at 40 kV. Structural evolution of the powder was evaluated using differential scanning calorimetry and thermogravimetric analyses (DSC/TGA, Pyris Diamond DSC/TG/DTA, Perkin-Elmer, USA) in nitrogen atmosphere with a heating rate of 10 °C/min. Two heating-up processes were employed to eliminate heat history of the feedstock powder. The contact angle measurement system (OCA20, Data physics, Germany) was adopted to measure contact angle of distilled water droplets and glycerol at room temperature. Roughness of the coatings was measured using surface profiler (Alpha-Step IQ, KLA Tencor, USA).

Corrosion resistance of the HDPE coatings, the copper coatings and the HDPE-Cu composite coatings was examined using neutral salt spray testing, which was performed according to the standard ASTM B117. Surface morphology, cross-sectional microstructure and corrosion products of exposed samples in salt spraying were examined periodically by FESEM. Electrochemical impedance spectroscopy (EIS)

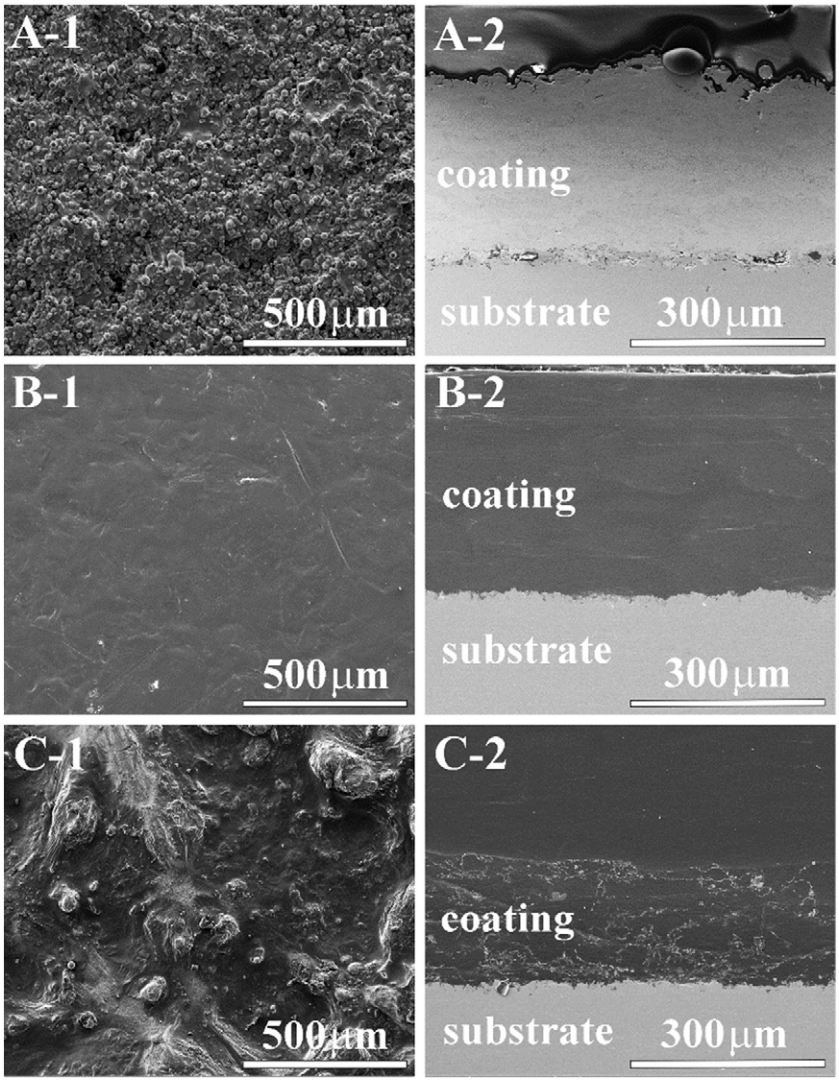

Fig. 3. Topographical (−1) and cross-sectional (−2) views of the pure Cu coating (A), the pure HDPE coating (B) and the HDPE-Cu coating (C).

spectra of the coatings were also assessed using a Solartron Modulab system (2100A, UK). All tests were conducted at room temperature in artificial seawater (ASW) prepared according to the standard ASTM D1141-98 (2003). Before the electrochemical measurement, the samples were immersed in an aerobic chamber containing ASW. Each measurement was repeated three times to ensure reproducibility. A traditional three-electrode cell was used, with 1 cm^2 platinum as the counter electrode, a saturated calomel electrode (SCE) as the reference electrode and the specimen with an exposed area of 1 cm^2 as the working electrode. EIS measurement was performed with an applied AC signal of 10 mV and the frequency ranging from 100 kHz to 0.01 Hz. After the measurement, the acquired data was fitted and analyzed using the software ZSimpWin.

Gram-positive *Bacillus* sp. (MCCC No. 1A00791) was typically used in this study. Adhesion of bacterial biofilm and further antibacterial efficiency were assessed. The coatings were immersed in the bacteria-containing ASW for 3 days. During the testing, peptone with a concentration of 3 g/L was added into the solution as carbon and energy sources for the bacteria. For FESEM observation of the bacteria colonized on the surfaces of the samples, the bacteria after incubation were fixed in 2.5% glutaraldehyde for 24 h, followed by gradual dehydration and coating with Au. The release rate of copper ions in 3.5 wt.% NaCl solution as a function of immersion time (up to 21 days) was also evaluated, and the concentration of copper ions was measured using inductively coupled plasma optical emission spectrometer (ICP-OES, PE Optima 2100DV, Perkin-Elmer, USA). Surface morphology and cross-sectional microstructure of the coatings were further characterized using FESEM.

3. Results and discussion

The starting HDPE particles show an ellipsoidal shape and $d_{0.5}$ is 85 μm (Fig. 2A). It is clear that after plating, the HDPE particles are entirely wrapped by thin copper layers (Fig. 2B) since copper tends to nucleate and grow on Ag catalytic sites that have already affiliated on the surfaces of individual HDPE particles. The cross-sectional views of the individual particle and corresponding EDS analyses further evidence the enwrapped structural features (Fig. 2C). It is also found that the homogeneously distributed copper layer is 1.1 ± 0.4 μm in thickness. That certain surface areas without copper coverage should be presumably due to the failure in absorbing Ag as the catalytic sites. The coverage of copper can be adjusted by controlling synthesis time.

Table 1
Thermal properties of the powder and the coatings.

Samples	T_m (°C)	$T_{5\%}$ (°C)	$T_{d(\max)}$ (°C)	ΔH_m (J·g^{-1})	χ_c (%)
HDPE powder	132.2	395.4	462.7	142.1	52.6
HDPE-Cu powder	132.4	408.7	474.8	103.3	38.2
HDPE coating	126.5	390.9	467.4	168.3	62.3
HDPE-Cu coating	129.6	376.3	461.5	168.8	62.5

T_m: melting temperature, $T_{5\%}$: temperature at 5% weight loss, $T_{d(\max)}$: maximum decomposition temperature, ΔH_m: melting enthalpy, and χ_c: degree of crystallinity of HDPE.

The coatings were fabricated by flame spraying. Surface morphology of the copper coatings, the HDPE coatings and the composite coatings are shown in Fig. 3A-1, B-1 and C-1, respectively. Similar to traditional flame sprayed polymer coatings [12], the HDPE-Cu composite coatings exhibit rough surfaces (Fig. 3C-1). The surface roughness R_a of the composite coating (1.08 ± 0.10 μm) is higher than that of the HDPE coating (0.22 ± 0.02 μm), which is likely due to the coarse nature of the copper shells. On the other hand, this suggests that the copper layer sticks to HDPE particle regardless of fully or partially melted state of the composite particles during spraying. The cross-sectional microstructures of the coatings are shown in Fig. 3A-2, B-2 and C-2. The dense structures have been achieved, and no marked flaws for instance microcracks or pores are seen from either the surfaces or the cross-sections of the coatings. It is exciting to note even distribution of copper in the coatings, and copper exists at the interfaces between individual HDPE splats (Fig. 3C-2). The content of copper in the inner and on the surface of the coating was examined using the software Image [21]. It is found that the content of copper on the surface of the coatings (35.11 ± 2.63 vol.%) is higher than that in the inner of the coatings (9.57 ± 1.28 vol.%), which suggests that higher release rate of Cu ions could be expected in the beginning of service.

XRD detection suggests the complete reaction of Ag catalytic sites with copper ions in the solution after electroless plating (Fig. 4A). No extra peaks are seen except those for copper and HDPE, indicating negligible oxidation or other undesirable chemical changes during spraying. Thermal analyses (TG and DSC) results of the original powder and the coatings are shown in Fig. 4B, C, D and Table 1. In the table, $T_{5\%}$ refers to the temperature at 5% weight loss of the composite coating, and

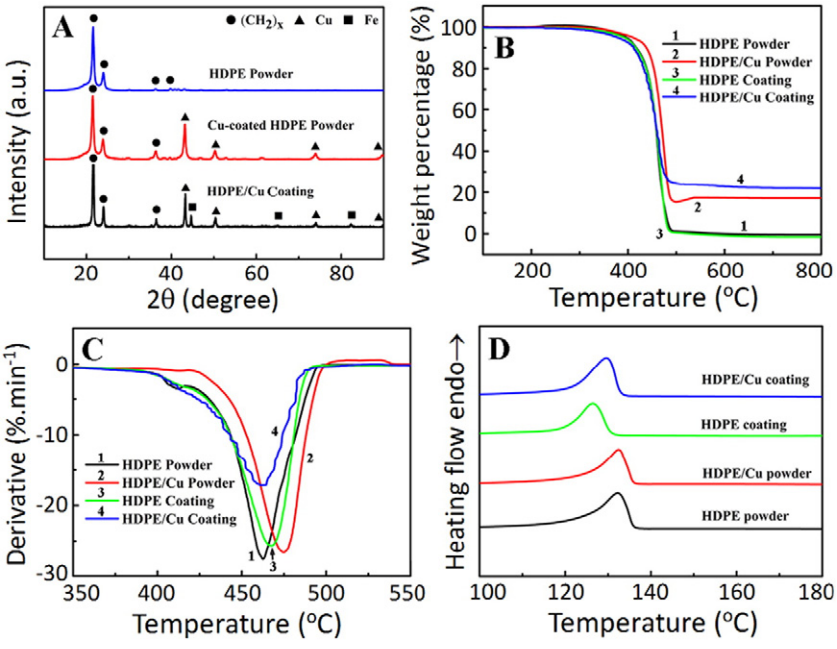

Fig. 4. XRD spectra (A), TG curves (B), DTG curves (C) and DSC curves (D) of the powder and the coating.

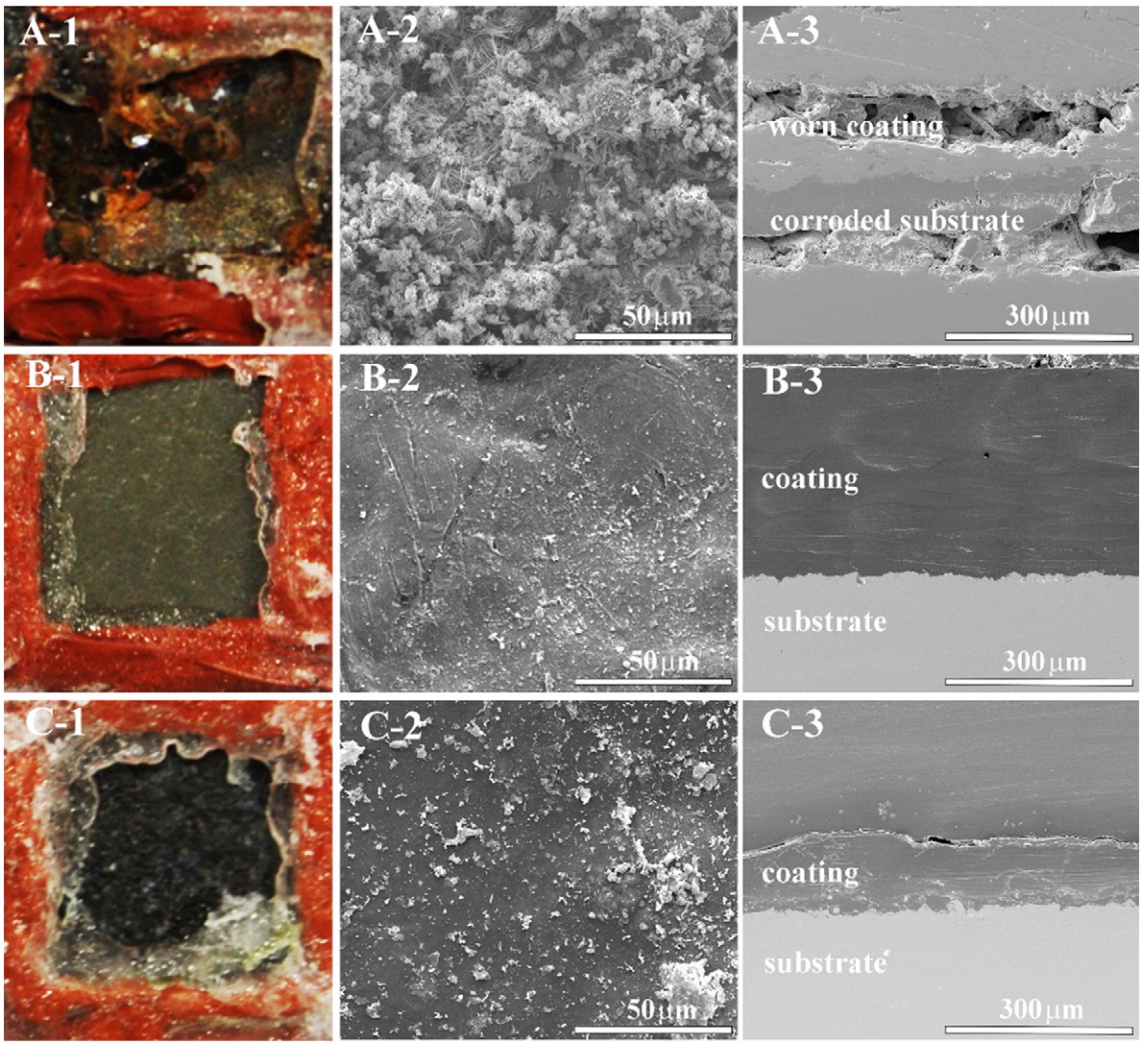

Fig. 5. Surface and cross-sectional microstructures of the copper coating (A), the HDPE coating (B), and the HDPE-Cu composite coating (C) after the salt spray testing for 14 days.

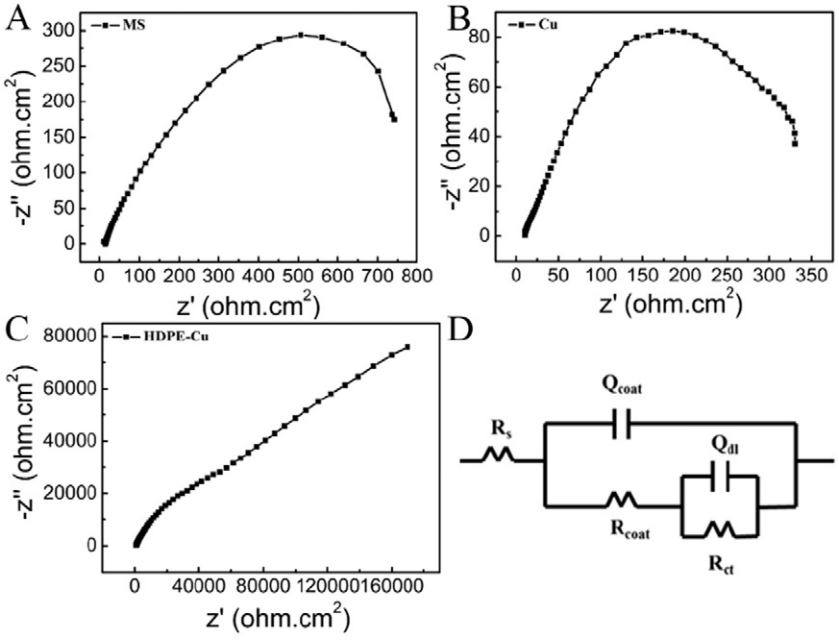

Fig. 6. Nyquist plots of the uncoated MS (A), the Cu coating (B), the HDPE-Cu coating (C) in ASW solution, and the equivalent circuit of the Cu coating and the HDPE-Cu coating (D).

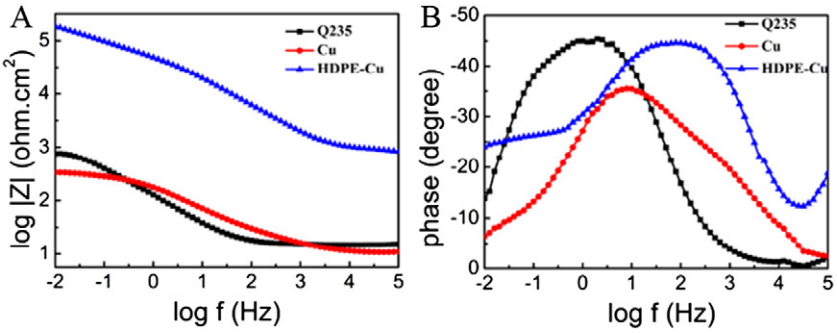

Fig. 7. Bode plots of the HDPE-Cu coating, the Cu coating and the uncoated MS in ASW solution.

$T_{d(\max)}$ is assigned to the maximum decomposition temperature of the coating. It is realized that the melting temperature of HDPE in the coatings decreases slightly as compared to that in the starting powder, which is probably due to thermal decomposition during spraying [22]. Higher $T_{5\%}$ and $T_{d(\max)}$ of HDPE in the Cu-coated HDPE powder compared to the HDPE powder is presumably attributed to the probability that the copper shell absorbs heat during the heating-up process. Interestingly, it is worth noting that for the HDPE-Cu composites, the coatings exhibit remarkable decrease in both $T_{5\%}$ and $T_{d(\max)}$, suggesting that the copper shell likely promotes thermal decomposition of HDPE during the coating fabrication. This could be explained by the prolonged heating effect exerted by the metallic layer to HDPE happened mainly during the flattening stage. Pretreatment of the starting HDPE for preparing the HDPE-Cu powder results in decreased crystallinity. However, it is noted that the crystallinity of HDPE in the coatings significantly augments compared to the starting HDPE powder. Presence of copper obviously facilitates the increased crystallinity. During flame spraying, the flattened particles were heated by both the flame and the subsequently impacted particles. This heating phenomenon could be considered as an annealing process for the copper shells and the HDPE cores, as a consequence the crystallinity of the HDPE particle in the composite coating increases distinctly. Enhanced strength could be expected for the coatings since the increase in crystallinity of HDPE gave rise to enhanced properties [23].

The anti-corrosion performance persists as one of the major challenges for nowadays available antifouling coatings for marine applications. In this study, corrosion resistance of the coatings was assessed by the neutral salt spray testing and potentiodynamic polarization, EIS spectra and equivalent circuit model were investigated. For the neutral salt spray testing, the coatings were exposed in salt spraying fog for up to 14 days. It is realized that after 6 h exposure, corrosion products of pure copper coatings are observed. 7 days exposure of the copper coatings results in full coverage of the corrosion products on the coating surfaces namely Fe_3O_4 and α-FeOOH (Fig. 5A), whereas the other samples are not corroded yet. After 14 days exposure to the corrosive media, the surface and the cross-section of the HDPE-based coating still exhibit intact state (Fig. 5B, C), suggesting favorable anti-corrosion performances. Electrochemical testing was also conducted to further assess the corrosion resistance of the substrate, the Cu coating and the HDPE-Cu composite coating in ASW solution. Nyquist plots for the samples are shown in Fig. 6A, B and C. The highest resistance value was obtained for the HDPE-Cu coating while the lowest resistance value was obtained for the Cu coating. The dense structure of the HDPE-Cu coating plays as a good barrier to the substrate, in turn restricting the diffusion of aggressive electrolyte species toward the substrate. In addition, the impedance spectra of the samples are represented in the forms of Bode plots (Fig. 7). It is clear that the HDPE-Cu coating shows increased maximum impedance modulus value |Z| (Fig. 7A) and maximal phase angle value (Fig. 7B), suggesting better corrosion resistance than the other samples.

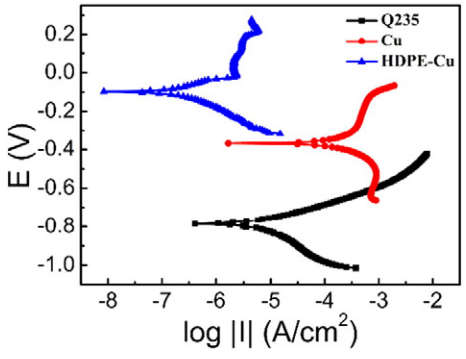

Fig. 8. Potentiodynamic polarization curves of the HDPE-Cu coating, the Cu coating and the uncoated MS in ASW solution.

The potentiodynamic polarization curves for the samples are shown in Fig. 8. The electrochemical corrosion parameters such as corrosion potential (E_{corr}) and corrosion current density (I_{corr}) are summarized in Table 2. The corrosion current density of the HDPE-Cu coating is 1.304×10^{-7} A/cm^2, much lower than the other samples. Furthermore, the polarization curves show positive shift in the corrosion potential for the HDPE-Cu coating. Corrosion potential is a measure of the tendency of the sample to corrode. The positive shift in corrosion potential suggests promising corrosion resistance of the HDPE-Cu coating. The corrosion protection efficiency (PE) of the coating was calculated using the formula [24]: $PE(\%) = \frac{I_{corr,bare} - I_{corr,coated}}{I_{corr,bare}} \times 100\%$, where $I_{corr,bare}$ and $I_{corr,coated}$ are the corrosion current density of the bare carbon steel and the coating, respectively. The protection efficiency of the HDPE-Cu coating is 96%.

The equivalent circuit model of the copper coating and the HDPE-Cu coating was fitted, and the results are shown in Fig. 6D and Table 3. The model consists of three parts: (1) solution resistance R_s; (2) parallel combination of the capacitance of the coatings Q_{coat} and the resistance of the coating R_{coat}; (3) parallel combination of double layer capacitance Q_{dl} and charge transfer resistance R_{ct}. The results show that R_{ct} and R_{coat} of the HDPE-Cu coating are higher than that of the copper coating, which also suggests higher corrosion resistance of the HDPE-Cu coating. The result from the model is consistent with the ones acquired from the potentiodynamic polarization curves and the electrochemical impedance spectra.

Table 2
Electrochemical characteristics for the HDPE-Cu coating, the Cu coating, and the MS substrate in ASW solution.

Samples	Corrosion potential (E_{corr}) (V/SCE)	Corrosion current density (I_{corr}) (A/cm^2)
MS substrate	−0.785	3.276×10^{-6}
Cu coating	−0.368	9.604×10^{-5}
HDPE-Cu coating	−0.100	1.304×10^{-7}

Table 3
Electrochemical impedance parameters of the copper coating and the HDPE-Cu coating.

Sample	R_s ($\Omega \cdot cm^2$)	R_{ct} ($\Omega \cdot cm^2$)	R_{coat} ($\Omega \cdot cm^2$)	Q_{CT} ($\mu F \cdot cm^{-2}$)	n_1	Q_{coat} ($\mu F \cdot cm^{-2}$)	n_2
HDPE-Cu coating	773.60	4.09×10^5	6.58×10^4	1.75×10^{-5}	0.80	3.48×10^{-6}	0.80
Cu coating	10.44	338.40	131.00	1.34×10^{-3}	0.74	1.47×10^{-4}	0.55

The assessment to the antifouling properties of the HDPE-Cu coatings reveals significantly prohibited attachment of *Bacillus* sp. bacteria on their surfaces. It is noted that after 3 days exposure in the bacteria-containing ASW, the HDPE coatings show clear colonization of the bacteria (Fig. 9A). In contrast, the Cu-containing coatings and the copper coatings show the attachment of few bacteria (Fig. 9B and C), which is obviously owing to release of copper ions into the solution [25–27]. Extensive investigations have proposed many possible antifouling mechanisms of copper ions [28]. Copper ions released from the Cu-containing coatings could engage with DNA of the bacteria and subsequently inhibit bacterial multiplication [27]. Copper ions adsorbed on cell surfaces could interact with caryon and cytoplasm of the bacteria cell, in turn damage cell membrane or destroy the function of bacterial enzymes [29,30]. For Cu-associated antifouling layers, the persistent challenge yet is how to control release of copper ions for long-term antifouling.

It is reported that the minimum concentration of copper ions to repel recruitment of *Bacillus* sp. and *E. coli* is 0.003 ppm [31]. The concentration of copper ion released from each sample was measured using ICP-OES. The concentration of copper ions as a function of immersion time could be examined in Fig. 9D. It is noted that the concentration of released copper ions exceeds the minimum required to repel the attachment of bacteria in all cases. In the first 3 days, the release rate of copper ions is relative high, simply because the volume percentage of Cu element on the coating surface is higher than that in the interior of the coating. In this stage, attachment of most microorganisms should be effectively inhibited. With further elongated incubation of the coating, release rate of copper ions decreases and reaches a relatively stable value, suggesting that the copper particles existing in the interior of the composite coatings begin to dissolve into NaCl solution. Image analyses from the surface and the cross-section of the coating incubated in the solution for 21 days (images not shown) reveal that the content of copper on the surface and the interior of the HDPE-Cu coating is 10.91 ± 3.17 vol.% and 9.15 ± 1.17 vol.%, respectively, which indicates that copper within the composite coatings do not easily dissolved into the solution in short time due to the protection of the inert polymeric matrix.

For marine applications of the coatings, their surface characteristics in particular surface wettability also play important roles in regulating their antifouling/anti-corrosion performances [32,33]. The results show that the water contact angle of the HDPE coating, the HDPE-Cu coating and the Cu coating is 92.8° ± 1.1°, 101.0° ± 1.1° and 135.9° ± 0.1°, respectively. The glycerol contact angle for the coatings shows a similar trend (data not shown). It is known that surface free energy and topology structure jointly contribute to the wettability [34]. Surface energy could be calculated by the equation proposed by Fowkes, Owens and Wendt [35]: $1 + \cos\varphi = 2\sqrt{\gamma_s^d}\left(\frac{\sqrt{\gamma_l^d}}{\gamma_l}\right) + 2\sqrt{\gamma_s^p}\left(\frac{\sqrt{\gamma_l^p}}{\gamma_l}\right)$, where φ is contact angle (degree), γ_s^p and γ_s^d are polar and dispersive component of free energy of the coating surface (mJ/m^2), γ_l is total free energy of the liquid (mJ/m^2) comprising polar energy γ_l^p and dispersive energy γ_l^d. Based on this equation, surface energy of the HDPE coating, the HDPE-Cu coating and the copper coating is 31.16 mJ/m^2, 38.67 mJ/m^2 and 3.17 mJ/m^2, respectively. It is surprising to note that the addition of copper into the HDPE coatings results in enhanced surface energy. The increase of surface wettability of the Cu-containing coatings is likely attributed to altered topology structure [32]. Surface roughness of the HDPE coating and the HDPE-Cu coating is 0.22 ± 0.02 μm and 1.08 ±

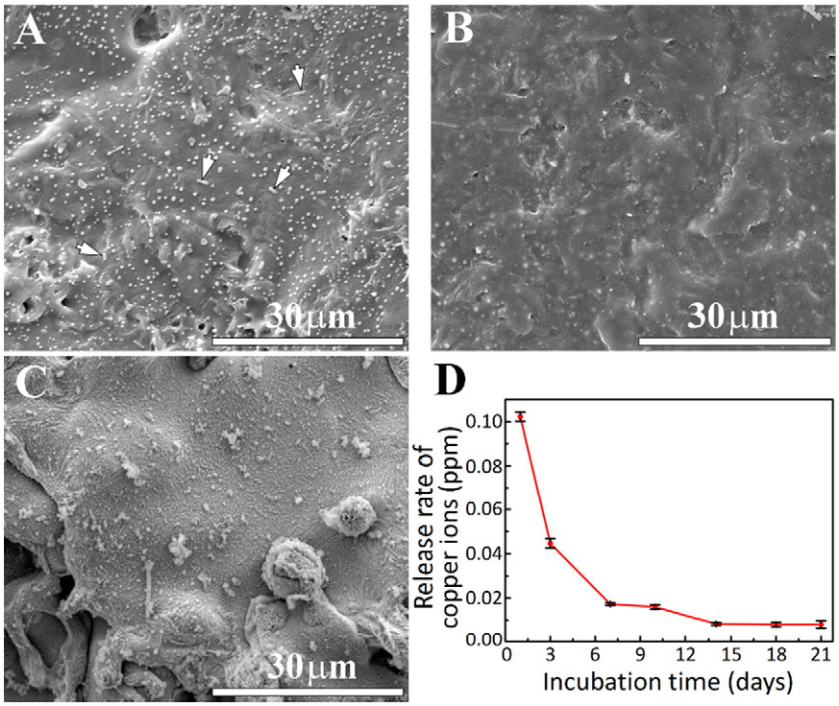

Fig. 9. Surface morphologies of the HDPE coating (A), the Cu coating (B) and the HDPE-Cu composite coating (C) after 72 h incubation in *Bacillus* sp. bacteria-containing ASW showing effective antifouling performances of the Cu-containing coatings. The white arrows point to typical *Bacillus* sp. bacterium. Release rate of copper ions from the HDPE-Cu coatings versus immersion time in 3.5 wt.% NaCl solution (D).

0.10 μm, respectively. The roughened surface introduced by the addition of copper could account for the enhanced wettability. The slightly enhanced hydrophobicity might promote antifouling performances of the constructed coating.

4. Conclusions

A new processing route for making HDPE-Cu powder and coatings was proposed. The flame sprayed HDPE-Cu coatings show a homogenous dense microstructure with unique distribution of copper at interfaces between individual HDPE splats. Both excellent antifouling and anti-corrosion performances were revealed for the Cu-containing composite coatings. The enwrapped coating structure offered controllable long-term release of copper ions from the coatings for inhibiting attachment and colonization of bacteria. The results shed light on potential applications of HDPE-Cu coatings for marine applications and the approach is effective for cost-efficiently making large-scale polymer-metal composite coatings for a variety of applications.

Acknowledgements

This research was supported by Project of Scientific Innovation Team of Ningbo (grant # 2015B11050), National Natural Science Foundation of China (grant # 31500772 and 41476064), China Postdoctoral Science Foundation (grant # 2014M561800 and 2016T90554), Key Research and Development Program of Zhejiang Province (grant # 2015C01036), International Scientific and Technological Cooperation Project of Ningbo (grant # 2016D10012) and 3315 Program of Ningbo.

References

[1] M. Legg, M.K. Yücel, I. Garcia de Carellan, V. Kappatos, C. Selcuk, T.H. Gan, Acoustic methods for biofouling control: a review, Ocean Eng. 103 (2015) 237–247.
[2] P. Buskens, M. Wouters, C. Rentrop, Z. Vroon, A brief review of environmentally benign antifouling and foul-release coatings for marine applications, J. Coat. Technol. Res. 10 (2013) 29–36.
[3] I. Banerjee, R.C. Pangule, R.S. Kane, Antifouling coatings: recent developments in the design of surfaces that prevent fouling by proteins, bacteria, and marine organisms, Adv. Mater. 23 (2011) 690–718.
[4] S.M. Olsen, L.T. Pedersen, M.H. Laursen, S. Kiil, K. Dam-Johansen, Enzyme-based antifouling coatings: a review, Biofouling 23 (2007) 369–383.
[5] E. Almeida, T.C. Diamantino, O. de Sousa, Marine paints: the particular case of antifouling paints, Prog. Org. Coat. 59 (2007) 2–20.
[6] D.M. Yebra, S. Kiil, K. Dam-Johansen, Antifouling technology - past, present and future steps towards efficient and environmentally friendly antifouling coatings, Prog. Org. Coat. 50 (2004) 75–104.
[7] W.Y. Bao, O.O. Lee, H.C. Chung, M. Li, P.Y. Qian, Copper affects biofilm inductiveness to larval settlement of the serpulid polychaete *Hydroides elegans* (Haswell), Biofouling 26 (2010) 119–128.
[8] S. Kuroda, J. Kawakita, M. Takemoto, An 18-year exposure test of thermal-sprayed Zn, Al, and Zn-Al coatings in marine environment, Corrosion 62 (2006) 635–647.
[9] R.J.K. Wood, A.J. Speyer, Erosion-corrosion of candidate HVOF aluminium-based marine coatings, Wear 256 (2004) 545–556.
[10] F.S. Rogers, Thermal spray for commercial shipbuilding, J. Therm. Spray Technol. 6 (1997) 291–293.
[11] K.J. Jothi, A.U. Santhoskumar, S. Amanulla, K. Palanivelu, Thermally sprayable anti-corrosion marine coatings based on MAH-g-LDPE/UHMWPE nanocomposites, J. Therm. Spray Technol. 23 (2014) 1413–1424.
[12] C.R.C. Lima, N.F.C. de Souza, F. Camargo, Study of wear and corrosion performance of thermal sprayed engineering polymers, Surf. Coat. Technol. 220 (2013) 140–143.
[13] A. Soveja, P. Sallamand, H. Liao, S. Costil, Improvement of flame spraying PEEK coating characteristics using lasers, J. Mater. Process. Technol. 211 (2011) 12–23.
[14] C. Zhang, G. Zhang, V. Ji, H. Liao, S. Costil, C. Coddet, Microstructure and mechanical properties of flame-sprayed PEEK coating remelted by laser process, Prog. Org. Coat. 66 (2009) 248–253.
[15] R. Ding, X. Li, J. Wang, L. Xu, Study on antifouling effect of cold spray Cu-Cu_2O coating, Paint Coat. Ind. 43 (2013) 1–6.
[16] P.C. King, A.J. Poole, S. Horne, R. de Nys, S. Gulizia, M.Z. Jahedi, Embedment of copper particles into polymers by cold spray, Surf. Coat. Technol. 216 (2013) 60–67.
[17] M.J. Vucko, P.C. King, A.J. Poole, C. Carl, M.Z. Jahedi, R. de Nys, Cold spray metal embedment: an innovative antifouling technology, Biofouling 28 (2012) 239–248.
[18] M.J. Vucko, P.C. King, A.J. Poole, Y. Hu, M.Z. Jahedi, R. de Nys, Assessing the antifouling properties of cold-spray metal embedment using loading density gradients of metal particles, Biofouling 30 (2014) 651–666.
[19] M.J. Vucko, P.C. King, A.J. Poole, M.Z. Jahedi, R. de Nys, Polyurethane seismic streamer skins: an application of cold spray metal embedment, Biofouling 29 (2013) 1–9.
[20] M. Narkis, J. Yacubowicz, A. Vaxman, A. Marmur, Electrically conductive composites prepared from polymer particles coated with metals by electroless deposition, Polym. Eng. Sci. 26 (1986) 139–143.
[21] V. Marcelino, V. Cnudde, S. Vansteelandt, F. Caro, An evaluation of 2D-image analysis techniques for measuring soil microporosity, Eur. J. Soil Sci. 58 (2007) 133–140.
[22] C. Li, T. Hou, X. She, X. Wei, F. She, W. Gao, L. Kong, Decomposition properties of PVA/graphene composites during melting-crystallization, Polym. Degrad. Stab. 119 (2015) 178–189.
[23] G. Dou, Q. Dou, Crystallization kinetics, spherulitic morphology, mechanical properties and heat resistance of β-nucleated impact-resistant propylene-ethylene copolymer, Thermochim. Acta 614 (2015) 21–32.
[24] E. Zampetti, S. Pantalei, S. Scalese, A. Bearzotti, F.D. Cesare, C. Spinella, A. Macagnano, Biomimetic sensing layer based on electrospun conductive polymer webs, Biosens. Bioelectron. 26 (2011) 2460–2465.
[25] S. Brooks, M. Waldock, The use of copper as a biocide in marine antifouling paints, advances in marine antifouling coatings and technologies, Antifouling Coat. Technol. 492–521 (2009).
[26] A.A. Finnie, D.N. Williams, Paint and coatings technology for the control of marine fouling, Biofouling 10 (2010) 185–206.
[27] T. Yuranova, A.G. Rincon, A. Bozzi, S. Parra, C. Pulgarin, P. Albers, J. Kiwi, Antibacterial textiles prepared by RF-plasma and vacuum-UV mediated deposition of silver, J. Photochem. Photobio. A Chem. 161 (2003) 27–34.
[28] J.L. Hobman, L.C. Crossman, Bacterial antimicrobial metal ion resistance, J. Med. Microbiol. 64 (2015) 471–497.
[29] X. Zhang, K.E. Aifantis, Interpreting the softening of nanomaterials through gradient plasticity, J. Mater. Res. 26 (2011) 1399–1405.
[30] P.C. Liu, J.H. Hsieh, C. Li, Y.K. Chang, C.C. Yang, Dissolution of Cu nanoparticles and antibacterial behaviors of TaN-Cu nanocomposite thin films, Thin Solid Films 517 (2009) 4956–4960.
[31] C.A. Kumar, S.R. Kumar, C.A. Prasun, A. Pulakesh, C. Ruchira, B. Tarakdas, A simple robust method for synthesis of metallic copper nanoparticles of high antibacterial potency against *E. coli*, Nanotechnology 23 (2012) 85103–85113.
[32] X. Chen, Y. Gong, X. Suo, J. Huang, Y. Liu, H. Li, Construction of mechanically durable superhydrophobic surfaces by thermal spray deposition and further surface modification, Appl. Surf. Sci. 356 (2015) 639–644.
[33] X. Chen, J. Yuan, J. Huang, K. Ren, Y. Liu, S. Lu, H. Li, Large-scale fabrication of superhydrophobic polyurethane/nano-Al_2O_3 coatings by suspension flame spraying for anti-corrosion applications, Appl. Surf. Sci. 311 (2014) 864–869.
[34] G. Godeau, C.R. Szczepanski, T. Darmanin, F. Guittard, Nanoparticle covered surfaces: an efficient way to enhance superhydrophobic properties, Mater. Des. 92 (2016) 911–918.
[35] M.A. Rahman, N. Soin, P. Maguire, R.A. D'Sa, S.S. Roy, C.M.O. Mahony, P. Lemoine, R. McCann, S.K. Mitra, J.A.D. McLaughlin, Structural and surface energy analysis of nitrogenated ta-C films, Thin Solid Films 520 (2011) 294–301.